

1 **Exploring Zoning Scenario Impacts upon Urban Growth Simulations Using a** 2 **Dynamic Spatial Model**

3 **Abstract**

4 Dynamic spatial models are being increasingly used to explore urban changes and evaluate
5 the social and environmental consequences of urban growth. However, inadequate representation
6 of spatial complexity, regional differentiation, and growth management policies can result in urban
7 models with a high overall prediction accuracy but low pixel-matching precision. Correspondingly,
8 improving urban growth prediction accuracy and reliability has become an important area of
9 research in geographic information science and applied urban studies. This work focuses on
10 exploring the potential impacts of zoning on urban growth simulations. Although the coding of
11 land-use types into distinct zones is an important growth management strategy, it has not been
12 adequately addressed in urban modeling practices. In this study, we developed a number of zoning
13 schemes and examined their impacts on urban growth predictions using a cellular automaton-based
14 dynamic spatial model. Using the city of Jinan, a fast-growing large metropolis in China, as the
15 study site, five zoning scenarios were designed: no zoning (S0), zoning based on land-use type
16 (S1), zoning based on urbanized suitability (S2), zoning based on administrative division (S3), and
17 zoning based on development planning subdivision (S4). Under these scenarios, growth was
18 simulated and the respective prediction accuracies and projected patterns were evaluated against
19 observed urban patterns derived from remote sensing. It was found that zoning can affect
20 prediction accuracy and projected urbanized patterns, with the zoning scenarios taking spatial
21 differentiation of planning policies into account (i.e., S2–4) generating better predictions of newly
22 urbanized pixels, better representing urban clustered development, and boosting the level of spatial
23 matching relative to zoning by land-use type (S1). The novelty of this work lies in its design of
24 specific zoning scenarios based on spatial differentiation and growth management policies and in

25 its insight into the impacts of various zoning scenarios on urban growth simulation. These findings
26 indicate opportunities for the more accurate projection of urban pattern growth through the use of
27 dynamic models with appropriately designed zoning scenarios.

28 **Keywords :** urban growth simulation; zoning scenarios; cellular automaton models; spatial
29 matching; prediction accuracy

30

31 Corresponding author. Email addresses:fanhuakong@163.com (F.Kong)

32

33 **1. Introduction**

34 The past few decades have witnessed a rapid growth in both the world's urban population and
35 the amount of built-up land, particularly in a number of developing countries. This has led to
36 significant changes in Earth's land surface that threaten the integrity of global ecosystems (Rafiee
37 et al., 2009). For example, although the proportion of people living in cities in China more than
38 tripled between 1978 and 2015, the urban built-up land coverage increased by nearly seven times
39 over the same period (The Yearbook of China's Cities, 2015). Rapid urban land expansion has
40 become the primary form of land-use change in China and has prompted concerns over loss of
41 large areas of high-quality farmland and primary forest, inadvertent climate repercussions, and
42 degradation in the overall quality of life (Ma et al., 2014; Song et al., 2015).

43 Urban growth is a complex, dynamic process that is driven by multiple biophysical and socio-
44 economic factors (Irwin et al., 2009; Akun et al., 2014; Maimaitijiang et al., 2015; Shafizadeh-
45 Moghadam and Helbich, 2015). Land-use change models can be used to explore urban growth and
46 land-use change dynamics to aid planners and resources managers in understanding land-use
47 changes and their potential socio-ecological consequences under different constraints (Yang and
48 Lo, 2003; Liu et al., 2008). Over the years, various land-use change models have been developed,
49 a number of which are suitable for urban growth simulation,. These include statistical models (e.g.,
50 Hu and Lo, 2007), artificial neural network models (e.g., Liu and Seto, 2008), cellular automaton
51 (CA) models (e.g., Clarke et al., 1997; Arsanjani et al., 2013; Chowdhury and Maithani, 2014;
52 Aburas et al., 2016; Ku, 2016), and agent-based models (e.g., Matthews et al., 2007; Valbuena et
53 al., 2010). Whereas statistically-based models are generally static in nature and more appropriate
54 for diagnostic or prescriptive applications, cellular automaton- and agent-based models are
55 dynamic and can be used for exploring future urban development under different constraints
56 (Torrens, 2011).

57 In this paper, we look primarily at urban cellular automaton models based on their capability
58 for exploring urban dynamics and on their general popularity (Torrens, 2011). Cellular automation

59 models simulate land cover or land use change using a set of rules which regulate cell (pixel)
60 conversions depending on their location, spatial relationships with other cells and various
61 landscape constraints. A well-known example of an urban cellular automata model is the Slope,
62 Land-use, Exclusion, Urban extent, Transportation, and Hillshade (SLEUTH) model, which has
63 been widely applied in urban growth prediction and forecasting (e.g., [Clarke et al., 1997](#); [Clarke](#)
64 [and Gaydos, 1998](#); [Silva and Clarke, 2002](#); [Herold et al., 2003](#); [Jantz et al., 2003, 2010](#); [Yang and](#)
65 [Lo, 2003](#); [Berling-Wolff and Wu, 2004](#); [Al-shalabi et al., 2012](#); [Onsted and Chowdhury, 2014](#)). At
66 the same time, despite their successful track record of application and high overall accuracy,
67 cellular automaton models can suffer from low pixel-matching precision (i.e., low local-scale
68 precision) ([Jantz et al., 2003](#)). Thus, improving urban growth prediction accuracy and reliability
69 has become an important area of research in geographic information science and applied urban
70 studies ([Torrens, 2011](#); [Brown et al., 2013](#); [Liu and Yang, 2015](#)). Although much progress has been
71 made in developing more technologically sophisticated urban cellular automaton models, there
72 have been some persistent challenges to the applicability of these models in reproducing patterns
73 resembling real cities, driven primarily by limitations on the availability of spatial data at required
74 resolutions and difficulties in representing spatial complexity, regional differentiation, and growth
75 management policies (see [Yang and Lo, 2003](#); [Torrens, 2011](#); [Liu and Yang, 2015](#)).

76 The focus of this paper is the sensitivity of urban growth to development planning policies,
77 which are important in urban growth management but have not been adequately addressed in urban
78 modeling practices (e.g., [Clarke et al., 1997](#); [Silva and Clarke, 2002](#); [Berling-Wolff and Wu, 2004](#);
79 [Lahti, 2008](#); [Wu et al., 2009](#)) due to difficulties in incorporating such development policies into
80 the conversion rules used by cellular automaton-based urban models (see [Torrens, 2002](#)). One way
81 to address this issue is to use an exclusion layer to indirectly integrate various development policies
82 into the simulation process (e.g., [Jantz et al., 2003](#); [Silva et al., 2008](#); [Akin et al., 2014](#)). However,
83 this approach has had only limited success to date because other issues, including spatial
84 complexity and regional differentiation, must be considered along with planning policies (e.g.,

85 [Goldstein et al., 2004](#)).

86 Urban planners often use zoning to differentiate land-use types as a method for controlling
87 and guiding the growth and changes in urban land use ([Onsted and Chowdhury, 2014](#)). This top-
88 down growth control and management approach has been widely adopted in the developed world
89 and is now being applied in a number of developing countries, including China ([Tian and Shen,](#)
90 [2011](#); [Long et al., 2012](#)). In China, all levels of government play very important roles in making
91 urban development policies and in building urban public service facilities and infrastructures. A
92 notable example of this is the establishment of several special economic zones by the central
93 government in the early 1980s as part of the country's economic reforms and policy of opening to
94 the world. These economic zones have profoundly affected urban growth patterns in the country
95 and made it necessary to consider zoning in urban growth modeling.

96 Several studies have recognized the implications of zoning for urban expansion simulations
97 and have noted how the appropriate use of zoning information can help improve simulation
98 accuracy ([Clarke et al., 1997](#); [Onsted and Chowdhury, 2014](#)). In this paper, “zone” is a term used
99 to refer to any subdivision of the landscape and can categorize divisions by land-use type,
100 administrative division, development planning subdivision, etc. Despite its advantages, zoning has
101 rarely been incorporated in urban modeling practices because its ability to significantly affect the
102 modeling outcomes has been generally disregarded or considered too difficult to demonstrate
103 ([Onsted and Chowdhury, 2014](#)). For example, in a study by [Lahti \(2008\)](#) the SLEUTH model, a
104 cellular automaton-based dynamic urban model, was successful in capturing bottom-up ecological
105 processes but could not adequately reproduce top-down phenomena due to its difficulty in
106 establishing a connection between bottom-up-oriented conversion rules and top-down urban
107 development policies. In other studies, SLEUTH was found to be incapable of thoroughly
108 capturing the characteristics of urban growth for various administrative divisions even when
109 zoning was taken into account (e.g., [Wu et al., 2009](#)). It should be noted that in these previous
110 studies zoning information was generally derived from either large administrative divisions (e.g.,

111 Wu et al., 2009) or land-use types (e.g., Berling-Wolff and Wu, 2004; Rafiee et al., 2009; Jantz et
112 al., 2010).

113 The aim of this study was to explore the potential impacts of zoning on urban growth
114 prediction and forecasting using the SLEUTH cellular automaton-based dynamic spatial model.
115 SLEUTH was selected for the study because of its flexibility, openness, non-linearity, and adaptive
116 ability (Clarke et al., 1997; Clarke and Gaydos, 1998). Using a set of urban growth rules, the
117 SLEUTH model can simulate complex urban growth dynamics. The model can be calibrated using
118 historical urban expansion data to obtain the best possible coefficient combinations. Detailed
119 discussion on model design and implementation procedures can be found in previous studies (e.g.,
120 Clarke et al., 1997; Clarke and Gaydos, 1998; Silva and Clarke, 2002; Herold et al., 2003; Yang
121 and Lo, 2003). Because of its rapid growth during the past several decades, the city of Jinan,
122 Shandong Province, China was selected as the study site. Several distinct zoning scenarios based
123 on land-use type, urbanization suitability, administrative division, and development planning
124 subdivision were carefully designed and used to simulate urban growth. Based on the model results,
125 the potential impacts of zoning were examined. Specifically, two questions were addressed: (1)
126 Would zoning affect urban growth prediction accuracy and projected urbanized patterns? and (2)
127 Which zoning scheme would allow the urban growth model to generate more accurate outcomes?
128 The findings of this study provide a valuable reference for addressing zoning information in urban
129 growth simulations and informing future urban planning and zoning policies.

130

131 **2. Study Area**

132 The study area represents a portion of Jinan, the capital city of Shandong Province in China.
133 Jinan lies between Taishan Mountain to the south and the Yellow River to the north (Figs 1 a, b).
134 The metropolitan area covers 8,117 km² and comprises seven districts—Shizhong, Tianqiao, Lixia,
135 Huaiyin, Licheng, Changqing, and Zhangqiu—and three counties—Pingyin, Jiyang, and Shanghe
136 (Fig. 1c). Jinan has experienced rapid growth in its urban population along with an expansion of

137 built-up land from 80.4 km² in 1949 to 383.3 km² in 2015 ([Statistical Year Book of Jinan, 2015](#)).

138 By the end of 2015, the total population of Jinan was 7.13 million, of whom 4.84 million were

139 urban residents. The city of Jinan formulated a primarily top-down regional planning strategy for

140 1996–2020 with the goal of promoting development toward the east, west, and north but restricting

141 development toward the south owing to the presence of Taishan Mountain. More specific urban

142 development plans were formulated in 2003, including development of a new district, old town

143 renovation, and urban expansion toward both the east and west. As a result, the city of Jinan now

144 comprises a central city and five development planning areas—East Metro, West Metro, Jibei

145 Metro, the airport development zone, and the southern mountain water conservation area ([Jinan](#)

146 [Municipal Planning Bureau, 2006](#)) ([Fig. 1d](#)). Rapid urban expansion in Jinan is closely related to

147 economic development, land-use policies, and physiographic characteristics. Although the

148 southern mountain area, serving as the water recharge area for the numerous springs in Jinan, has

149 been designated a key protected region, the mountain area as a whole has witnessed massive urban

150 expansion, which, in turn, has prompted an even stricter protection and development plan

151 specifically targeting the southern mountain area and the springs in the city. In addition, Jinan has

152 successively implemented a series of urban renewal projects and plans to create new districts. This

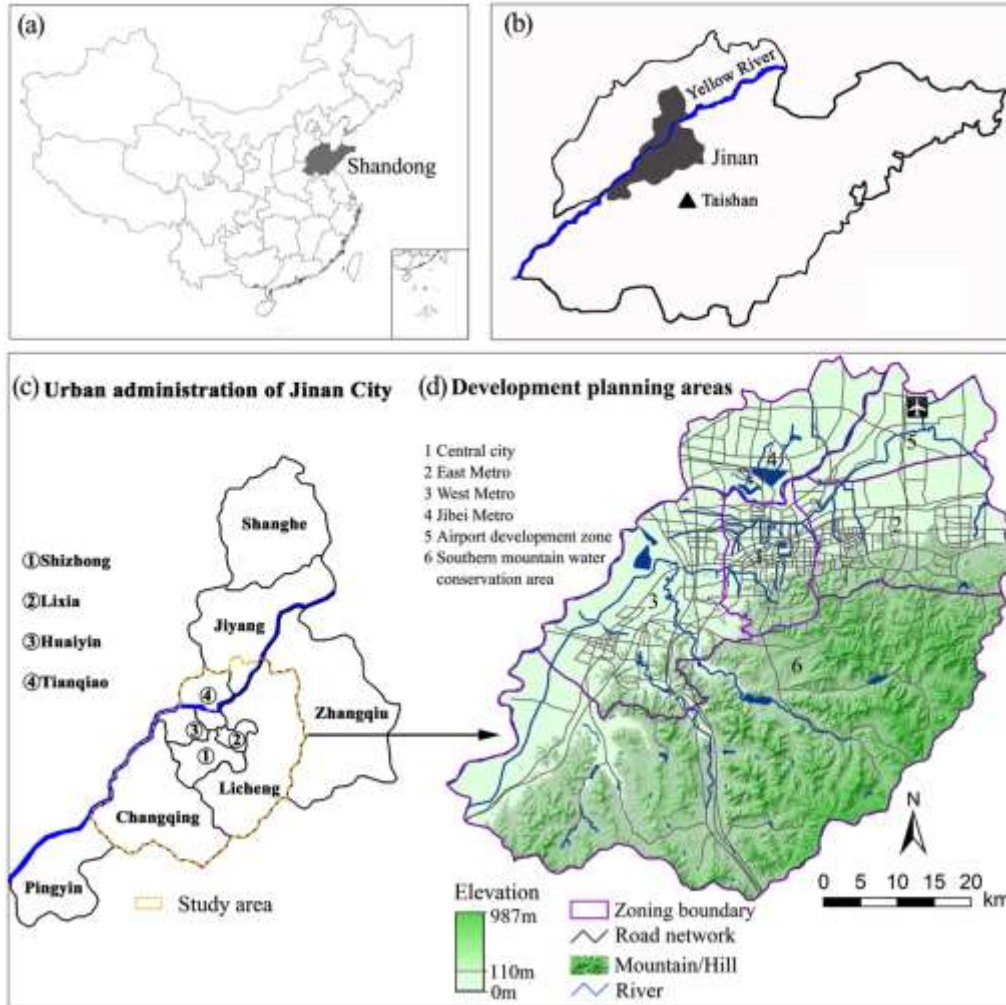
153 planning has collectively affected the magnitude and direction of urban growth. In this study, we

154 will specifically target an area of approximately 3,446 km² that includes the six districts under the

155 jurisdiction of Jinan and the Jibei metropolitan area in which the government and urban planners

156 have implemented different development policies that can affect future urban development ([Fig.](#)

157 [1d](#)).



158
159 Fig. 1 Location of the study area

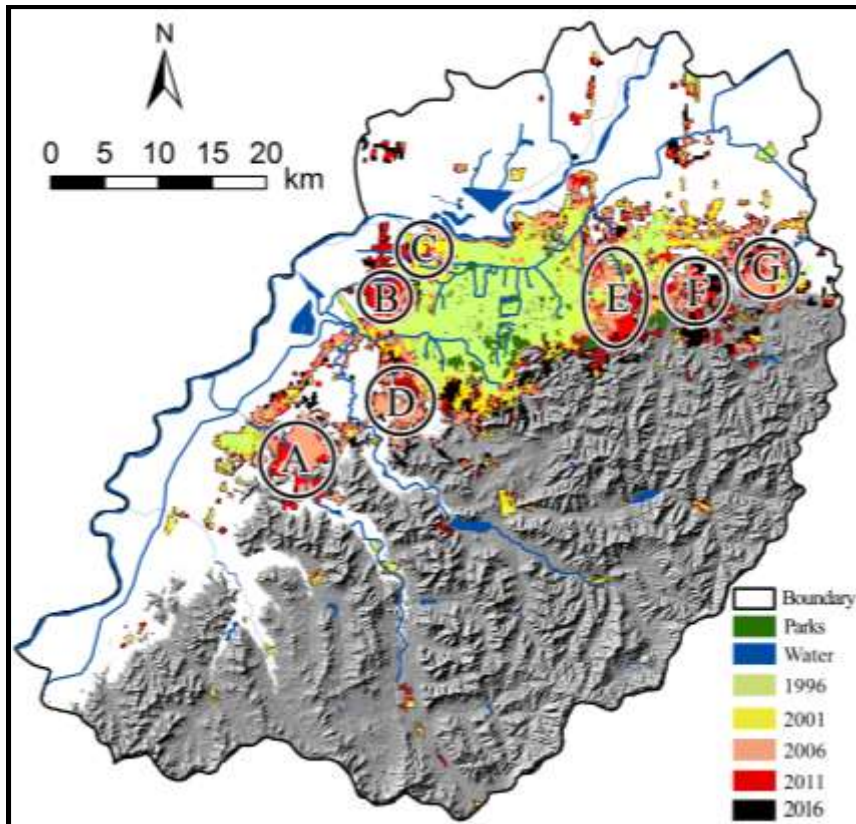
160 **3. Research Methods**

161 **3.1. Data acquisition and preprocessing**

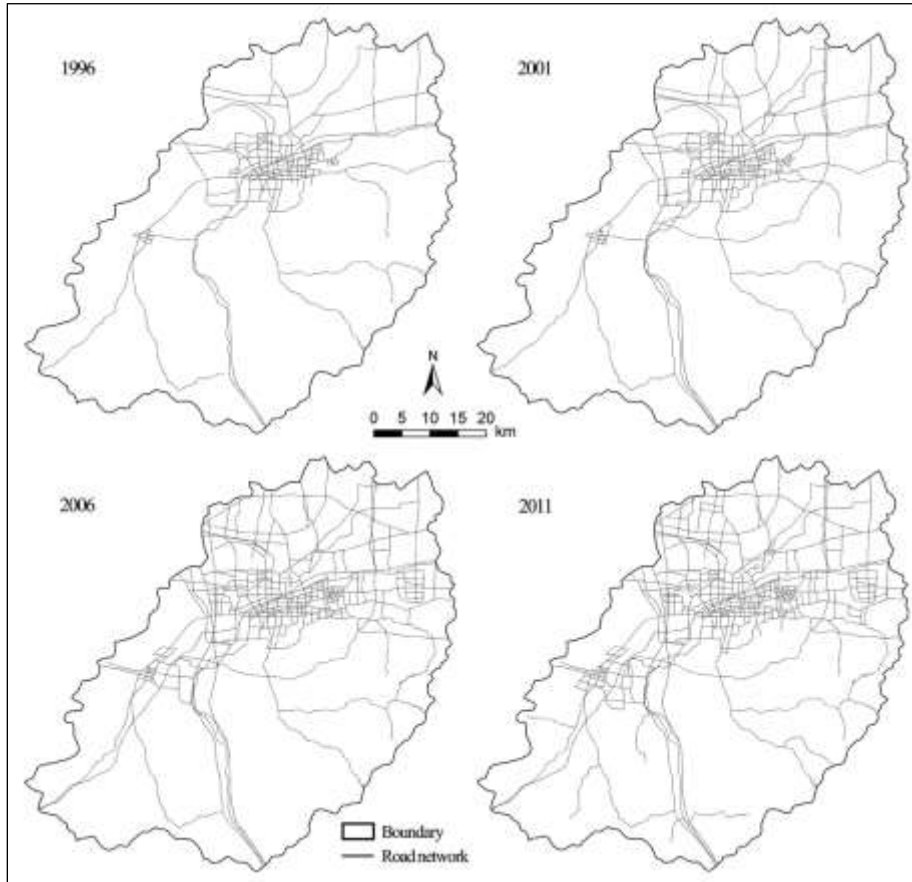
162 As mentioned earlier, the SLEUTH model was used to explore the impacts of zoning scenarios
 163 on urban growth simulations. This process involved the use of several datasets during various
 164 stages of model implementation: Landsat Thematic Mapper (TM) images collected in April 1996,
 165 July 2001, May 2006, and June 2011; Landsat 8 Operational Land Imager (OLI) images collected
 166 in May 2016 (which were used for validation only); topographic maps at 1:50,000; and various
 167 urban planning documents from the Jinan five-year development plans (1996–2000, 2001–2005,

168 2006–2010, 2011–2015, and 2016–2020) and Jinan master plans (2006–2020 and 2016–2020).

169 Data preprocessing was conducted as follows. First, a geometric correction procedure was
170 applied to the remote sensor images with root mean square (RMS) errors of less than one pixel. In
171 this procedure, the cubic convolution method was used for intensity interpolation between ground
172 control points (GCPs) selected uniformly across the study area. Second, each image was clipped
173 using the study site boundary and a supervised classification method was used to derive an urban
174 extent map from each of the Landsat TM and OLI images (Fig. 2). The overall classification
175 accuracy was found to be 93.2% as determined by error matrices and the Kappa index was found
176 to be 0.91. Finally, a road network dataset comprising an updated road map for each of four
177 different years, i.e., 1996, 2001, 2006, and 2011, was generated by manually digitizing the roads
178 visible in each TM image (Fig. 3).



179
180 Fig. 2 Spatial growth of urban extent in Jinan from 1996 to 2016. A-G: components of urban
181 growth regions

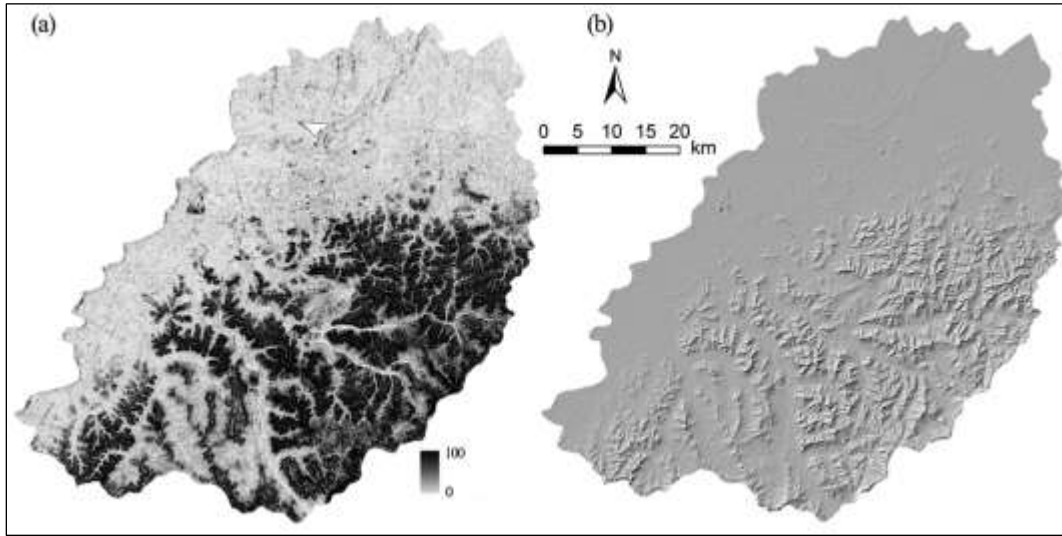


182

183 Fig. 3 Road network maps for 1996, 2001, 2006, and 2011

184 **3.2. Model input**

185 To run the SLEUTH 3.0 model, five data layers are required as inputs: urban extent,
 186 transportation, slope, hillshade, and an exclusion layer. In this study, the urban extent was a
 187 binary raster of urban and nonurban land use derived from the TM images (Fig. 2). The roads
 188 (transportation) were not weighted following Chaudhuri and Clarke (2013), who found no
 189 significant difference in results from road weighting. The slope and hillshade layers were generated
 190 from a digital elevation model (DEM) (Fig. 4), with the slope expressed as a percentage
 191 representing the ratio of vertical to horizontal change and cells with slopes greater than 100% (out
 192 of a possible slope index from 0 to ∞) assigned slope values of 100. The exclusion layer was
 193 defined based on specific scenarios discussed in Section 3.3. Finally, as required by the model all
 194 data were converted to GIF format with a cell size of 60 m \times 60 m.



195
 196 Fig. 4 Two model input layers: slope (a) and hillshade (b)

197 **3.3. Zoning scenarios**

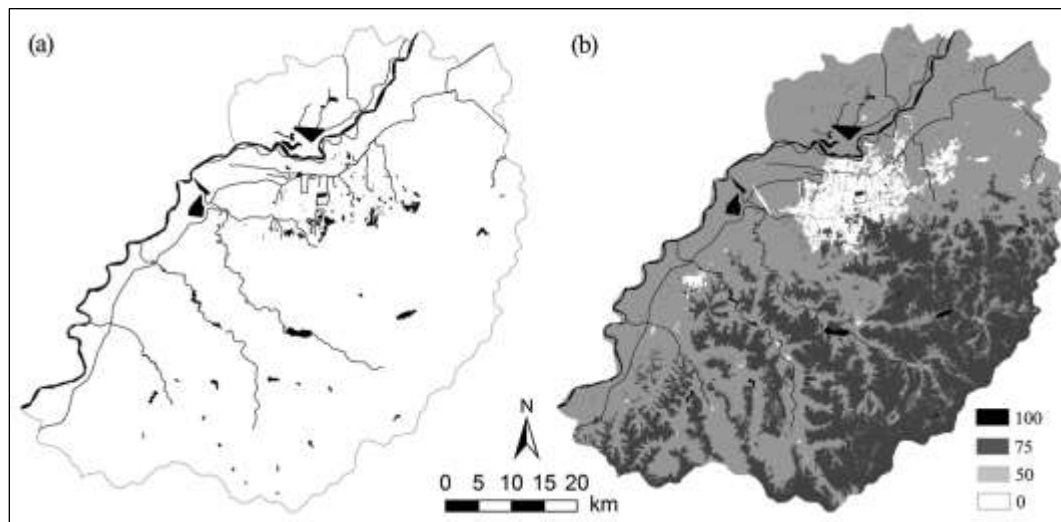
198 The SLEUTH model predicts future urban growth and land cover changes by modifying
 199 internal parameters or manipulating the exclusion layer in historical data. In this manner, SLEUTH
 200 can be used to support urban planning activities (Clarke et al., 1997, Clarke and Gaydos, 1998;
 201 Silva and Clarke, 2002; Jantz et al., 2003, 2010). The ability to relate the exclusion layer to specific
 202 land-use or policy constraints based on the integration of geographic information systems with
 203 remote sensor data is considered to be another important advantage of the SLEUTH model (Jantz
 204 et al., 2003).

205 In China, the top-down approach has been widely used in urban and regional planning, which
 206 can significantly affect urban growth patterns (Long et al., 2012; Tian and Shen, 2011), as is further
 207 discussed in the context of Jinan in Section 4.1. To explore the possible impacts of various zoning
 208 methods on urban growth simulation, we specifically designed five different zoning scenarios and
 209 prepared an exclusion layer for each of them.

210 **3.3.1 Scenario S0: No zoning**

211 Scenario S0 (no zoning) served as a benchmark for examining the potential impacts of specific
 212 land-use and development policies on urban growth simulations based on a comparison of its

213 outcomes with those of other scenarios. For S0, an exclusion layer comprising large water bodies
214 and parks (Figs. 2 and 5a) with assigned attribute values of 100 (complete preservation) was
215 created, following the methodology of previous studies (e.g., Silva and Clarke, 2002; Rafiee et al.,
216 2009; Akin et al., 2014).



217
218 Fig. 5 Exclusion layers used for Scenarios S0 (a) and S1 (b). Note that pixels with the attribute
219 value of 100 represent completely excluded areas

220 3.3.2 Scenario S1: Zoning based on land-use type

221 Zoning scenario S1 was designed to address the possible impacts of land-use policies by
222 assigning specific values to different land uses. For example, forest land was assigned a higher
223 value as it is generally more protected. User-defined options have often been used to value
224 specific land-use types and design exclusion layers (e.g., Jantz et al., 2003, 2010; Berling-Wolff
225 and Wu, 2004; Rafiee et al., 2009; Akin et al., 2014) even when zoning is not explicitly mentioned.
226 An exclusion layer was also generated as a user-defined option for S1 based on data on land-use
227 in 1996. Under S1, an attribute value of 100 was assigned to large water bodies and parks (as under
228 S0) and values of 75, 50, and 0 were assigned forests, agricultural areas, and areas with no
229 preservation rules, respectively (Fig. 5b). However, the scenario did not consider development
230 policies among different regions or spatial locations within a given land-use type.

231 3.3.3 Scenario S2: Zoning based on urbanization suitability

232 Zoning scenario S2 was based on the evaluation of urban growth suitability in terms of both
233 the impacts of land use and urban development policies related to protecting important natural and
234 ecological spaces and regional differentiation of urban growth potential owing to accessibility.
235 This methodology for designing exclusion layers was also used in a number of previous studies
236 regarding smart-growth (e.g., Jantz et al., 2010; Mahiny and Clarke, 2012) or ecologically
237 sustainable development scenarios (e.g., Jantz et al., 2003; Rafiee et al., 2009; Yin et al., 2015).

238 The exclusion layer under S2 was generated using a multi-factor overlay analysis of eight
239 thematic layers (Table 1), which were assumed to be the primary factors affecting land suitability
240 for urban growth based on situation within the study area and data availability as well as from
241 reference to previous studies (e.g., Mahiny and Clarke, 2012; Yin et al., 2015). The analytical
242 hierarchy process (AHP) method (Saaty, 1980) was used to weight the thematic factors (Table 1).
243 As factor five (proximity to rivers and water bodies) was a constraining factor, the minimum
244 overlay method was specially adapted to combine it with the other seven weighted factors.

245
246 **Table 1** Data layers used in the multi-factor overlay analysis for urbanized suitability assessment
247 and weights assigned to each of the seven factors

No.	Factor	Weight
1	Slope	0.114
2	Relief	0.114
3	Land use	0.051
4	Forest density	0.052
5	Proximity to rivers and water-bodies	–
6	Accessibility to urban edges	0.223
7	Accessibility to city centers	0.223
8	Accessibility to planned new district centers	0.223

248 Note: the “proximity to rivers and water bodies” was set as constraining factor

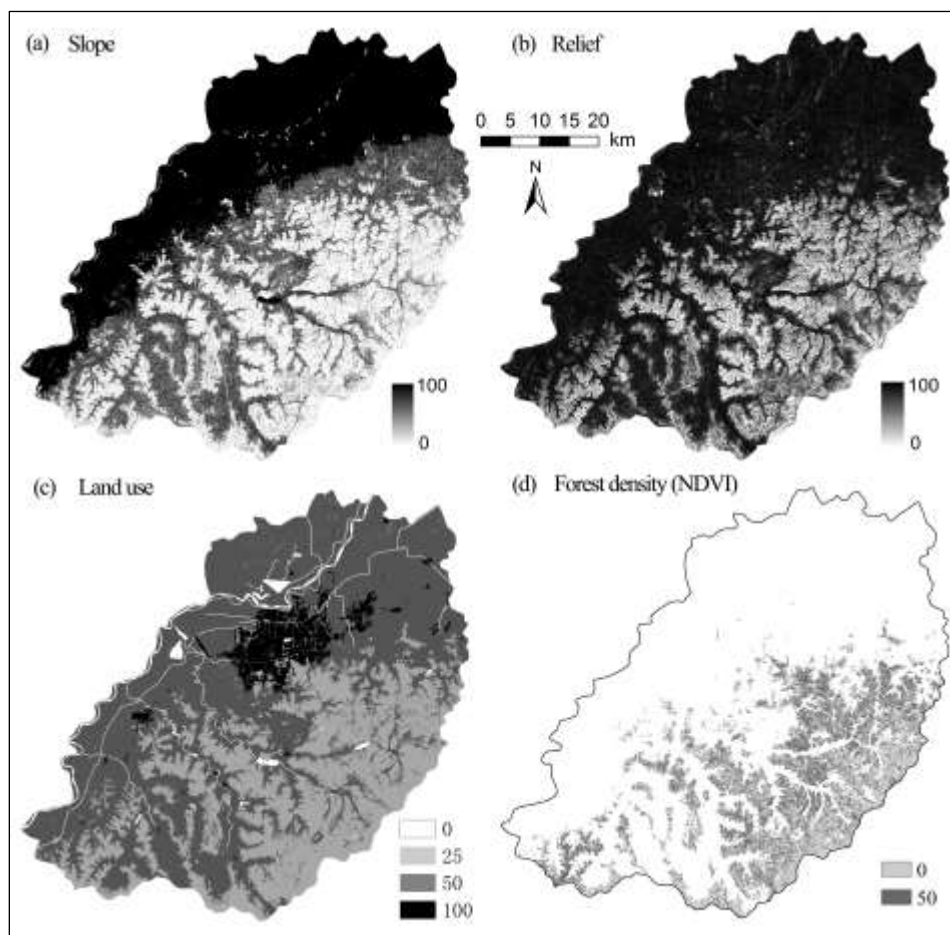
249 Topographic slope and relief are two important factors affecting urbanized suitability. In this
250 study, areas with slopes greater than 25% and/or reliefs of more than 40 m were considered

251 unsuitable for development and were assigned a value of zero. The values of other areas were
252 linearly fuzzified using a monotonically decreasing trend and normalized to a scale from 0 (least
253 suitable) to 100 (most suitable) (Fig. 6a, b). Fuzzy values for the five land-use categories were
254 defined through a user-defined option. To maintain consistency with the Scenario S1 schema,
255 attribute values of 0, 25, 50, and 100 were assigned to large water bodies and parks, forests,
256 agricultural areas, and areas that were absolutely suitability for urban growth, respectively (Fig.
257 6c). The normalized difference vegetation index (NDVI) was used to represent forest density, with
258 NDVI values greater than 0.45 assigned a value of 0, indicating an absolutely protected area that
259 should not be used for urban development, and those with NDVIs of less than 0.45 assigned a
260 value of 50 (Fig. 6d).

261 As a constraint factor, the distances to rivers and water bodies were also weighted through a
262 user-defined option. To protect water resources and riparian vegetation and prevent flood damage
263 to settlements, all rivers and water bodies and their respective buffer zone areas (200 m from the
264 Yellow River and 100 m from all other rivers and water bodies) were assigned a value of zero,
265 indicating restricted areas that were not suitable for urban growth.

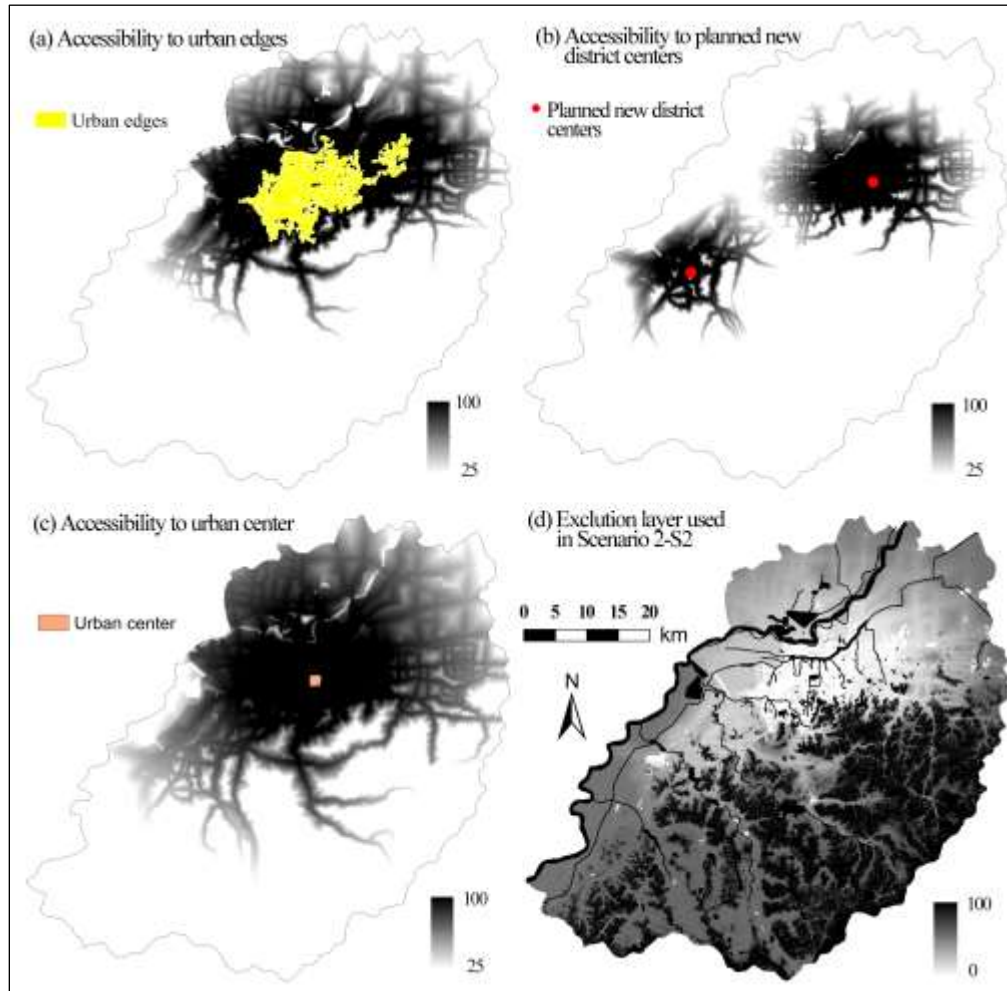
266 Accessibility to urban edges, urban centers, and planned new district centers are important
267 driving factors for urban growth (Hansen, 1959; Geurs and Van Wee, 2004). In this case,
268 accessibility can be defined as “the ease with which any land-use activity can be reached from a
269 location using a particular transport system” (Dalvi and Martin, 1976), which can be easily
270 calculated using the cost-distance method by any GIS software package such as ArcGIS (e.g.,
271 Kong et al., 2012). In this study, travel speed was defined as 40 km per hour and cost-distance as
272 15 min/10 km along all types of road in the road network. Areas with no roads were defined as
273 walking networks and assigned cost values according to three categories: rivers and water, 1,000;
274 mountains, 500; and others, 120. Three different levels of accessibility were also identified. If an
275 area’s accessibility to urban edges or planned new district centers was less than 10 min and that to
276 urban centers was less than 30 min, it was assigned 100 to indicate highest suitability. Similarly, if

277 the urban edge/planned new district center and urban center accessibilities were within 10–30 and
278 30–60 min, respectively, the accessibility values were linearly fuzzified using a monotonically
279 decreasing trend and normalized to 25–100. Accessibilities to urban edges and planned new district
280 centers urban centers greater than 30 and 60 min, respectively, resulted in an assigned value of 25
281 (low suitability) (Fig. 7a, b, c).



282
283 Fig. 6 Four factors used in multi-factor overlay analysis for urbanized suitability assessment

284 To yield an urbanized suitability map, an overlay operation was used to sum the weighted
285 factors. As the highest suitability corresponded to the lowest value in the excluded layer, the values
286 of urbanized suitability were, therefore, reversed with respect to the values in Scenario S1 (Fig.
287 7d).



288
 289 Fig. 7 Accessibility factors used in multi-factor overlay analysis for urbanized suitability
 290 assessment and the exclusion layer used in Scenario S2

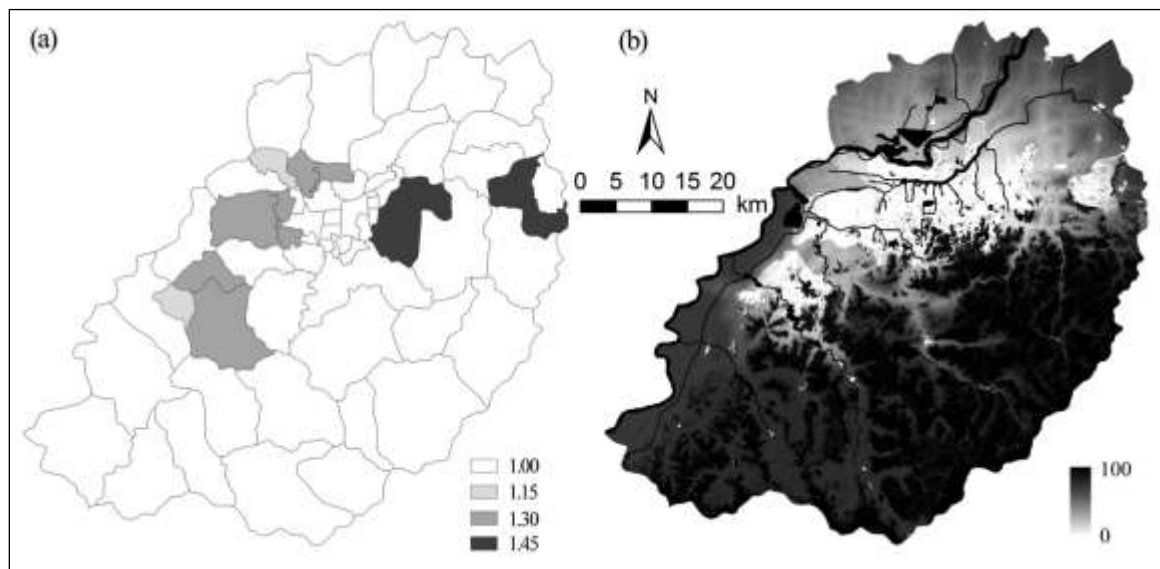
291 3.3.4 Scenario S3: Zoning based on administrative division

292 Zoning scenario S3 was used to assess urbanized suitability and the potential impacts of
 293 development policies on different administrative divisions. Different top-down development
 294 policies can result in different urban growth patterns (Yu and Ng, 2007); in this study, a
 295 development policy impact coefficient layer was created to represent such impacts, and the
 296 exclusion layer in Scenario S3 was derived by combining the urbanized suitability layer derived
 297 for Scenario S2 with this policy impact coefficient layer.

298 The study area was first subdivided based on the present administrative divisions. As some
 299 administrative divisions in downtown Jinan had already become completely urbanized and were

300 mostly adjacent to each another, these divisions were grouped into one division, resulting in a
301 study area comprising sixty divisions (Fig. 8a). To create the development policy impact
302 coefficient layer, the respective policies related to the expansion of urban land use were first
303 categorized. The primarily executive urban and regional development policies in Jinan are listed
304 in Table 2. These policies were then divided into four different levels (national, provincial,
305 municipal, district or below) and assigned the user-defined values of 1.45, 1.30, 1.15, and 1.00,
306 respectively (Table 2). Finally, urban growth areas were classified and assigned zoning values by
307 policy level to create the development policy impact coefficient layer. Using this layer, the
308 development policies in different administrative divisions could be evaluated with respect to
309 specific policy level (Fig. 8a).

310 A policy-restricted urban growth suitability layer for Scenario S3 was generated by
311 multiplying the urbanization suitability layer values for Scenario S2 with those of the respective
312 administrative division-based development policy impact coefficient layer areas (with all of the
313 resulting values larger than 100 set to 100). The values in the resulting layer were then reversed to
314 generate the final exclusion layer for Scenario S3 (Fig. 8b).



315

316 Fig. 8 Administrative division-based development policy impact coefficient layer (a) and exclusion
 317 layer used in Scenario S3 (b). Note that pixels with attribute values of 100 represent completely
 318 excluded areas

319

320 [Table 2](#) List of major urban and regional development policies for Jinan since 1996 and their
 321 respective policy levels

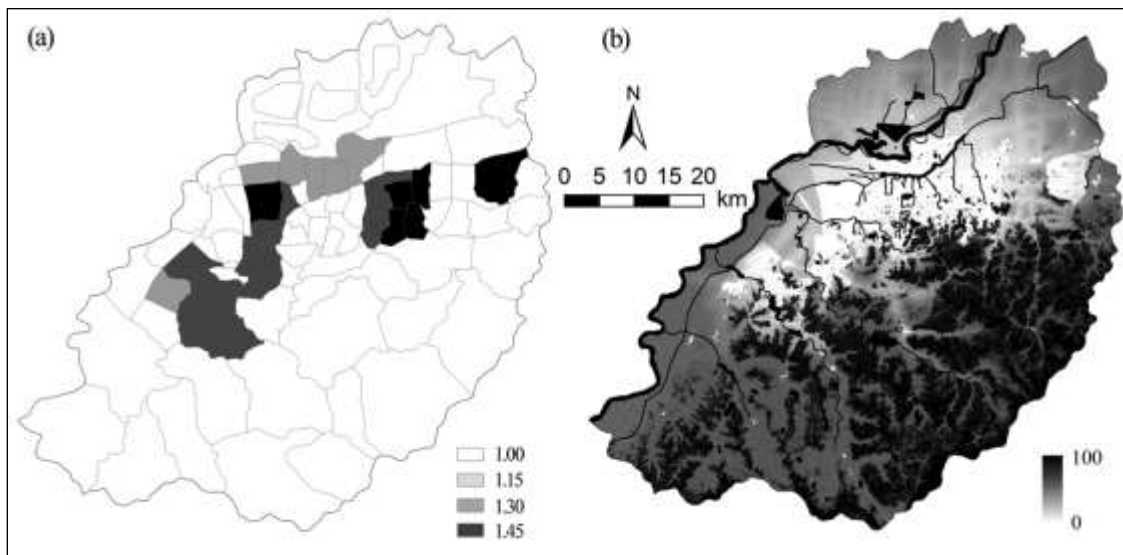
No.	Policy	Policy makers	Policy level	Weighted value
1	Jinan high and new technology industrial development zone (1991--)	Shandong provincial government (National level)	National	1.45
2	Jinan Economic Development Zone (1999--)	Shandong provincial government (Provincial level)	Provincial	1.30
3	Jinan ninth five-year development plan (1996–2000)	Jinan development and reform commission, Jinan Municipal government	Municipal	1.15
4	Jinan master planning (1996–2010)	Jinan municipal planning bureau	Municipal	1.15
5	Jinan big changes in five years (1997–2002)	Shandong provincial government Jinan municipal government	Provincial	1.30
6	Jinan tenth five-year development plan (2001–2005)	Jinan development and reform commission, Jinan Municipal government	Municipal	1.15
7	Jinan master planning (2006–2020)	Jinan municipal planning bureau	Municipal	1.15
8	Jinan eleventh five-year development plan (2006–2010)	Jinan development and reform commission, Jinan Municipal government	Municipal	
9	Jinan twelfth five-year development plan (2011–2015)	Jinan development and reform commission, Jinan Municipal government	Municipal	1.15
10	The main function zoning in Shandong province (2013)	Shandong provincial government Shandong provincial development and reform commission	Provincial	1.30
11	Jinan thirteenth five-year development plan (2016–2020)	Jinan development and reform commission, Jinan Municipal government	Municipal	1.15
12	Jinan master planning (2016–2020)	Jinan municipal planning bureau	Municipal	1.15
13	The ecological protection red line planning in Shandong province (2016–2020)	Shandong provincial government Environmental protection bureau of Shandong Province	Provincial	1.30

322 *Note: A series of district or below level policies were published in the past few years and have been
 323 weighted as “1” for this study.

324 3.3.5 Scenario S4: Zoning based on development planning subdivision

325 Zoning scenario S4 was developed as an extension of Scenario S2 to reflect the potential
 326 impacts of development policies on different planning subdivisions (functional groups). A detailed

327 planning scheme (Jinan Municipal Planning Bureau, 2006) defines six major functional areas in
328 Jinan, namely, the central area, the East Metro district, the West Metro district, the Jibei Metro
329 district, the airport development zone, and the southern mountain ecological conservation district
330 (Fig. 1d). The scheme also specifies eighty-four functional groups (Fig. 9a). Scenario S4
331 incorporates subdivisions additional to those in Scenario S3, particularly in the urban development
332 planning area, i.e., the East Metro, West Metro, and Jibei Metro districts (Fig. 8a, Fig. 9a). The
333 same data processing procedure used in Scenario S3 was used to create S4, with the generation of
334 a functional group-based development policy impact coefficient layer (Fig. 9a) followed by the
335 generation of an exclusion layer (Fig. 9 b).



336
337 Fig. 9 Functional group-based development policy impact coefficient layer (a) and exclusion layer
338 used in Scenario S4 (b). Note that pixels with attribute values of 100 represent completely excluded
339 areas

340 3.4. Model calibration

341 Urban model calibration is carried out to obtain sets of parameters that can be used to
342 accurately reproduce historical urban growth, which in turn enables the simulation of future urban
343 growth in support of land-use planning activities (Dietzel and Clarke, 2007; Akin et al., 2014). The
344 success of model simulation depends significantly on the calibration process (Silva and Clarke,

345 2002). In this study, a brute-force Monte Carlo method was used for model calibration in a three-
 346 step process of coarse, fine, and final calibration. The set of growth coefficients obtained in each
 347 step was used as input for the calibration in the next step, which progressively narrowed the range
 348 of each parameter. Each calibration involved several Monte Carlo experiments. Although
 349 comparison of experimental results such as these with data generated from remotely sensed images
 350 can generate series of statistics to quantify simulation accuracy, there remain controversies over
 351 which indices can best characterize the accuracy of a model (Clarke et al., 1997; Silva and Clarke,
 352 2002; Herold et al., 2003; Jantz et al., 2003; Onsted and Chowdhury, 2014). Here, the Optimal
 353 SLEUTH Metric (OSM), representing the product of seven metrics—Compare, Pop, Edges,
 354 Cluster, Slope, Xmean, and Ymean—was used for model calibration (Table 3). The selection of
 355 metrics was largely based on the research conducted by Dietzel and Clarke (2007), who found that
 356 these metrics are weakly correlated and can be used to quantify model simulation accuracy.

357

358 Table 3 Description of metrics used for evaluation of the calibration results (Dietzel and Clarke,
 359 2007).

Metric name	Description
Compare	Comparison of modeled final urban extent to real final urban extent
Pop	r^2 Population: Least-squares regression score of modeled urbanization compared with actual urbanization for control years
Edges	Edge r^2 : Least-squares regression score for modeled urban edge count compared with actual urban edge count for control years
Cluster	R^2 cluster: Least-squares regression score of modeled urban clustering compared with known urban clustering for control years
Slope	Average slope r^2 : Least-squares regression of average slope of modeled urbanized cells compared with average slope of known urban cells for control years
Xmean	X- r^2 ; Center of gravity [X]: Least-squares regression of average X values for modeled urbanized cells compared with average X values of known urban cells for control years
Ymean	Y- r^2 ; Center of gravity [Y]: Least-squares regression of average Y values for modeled urbanized cells compared with average Y values of known urban cells for control years
OSM	Optimal SLEUTH Metric, the product of the preceding seven indices

360

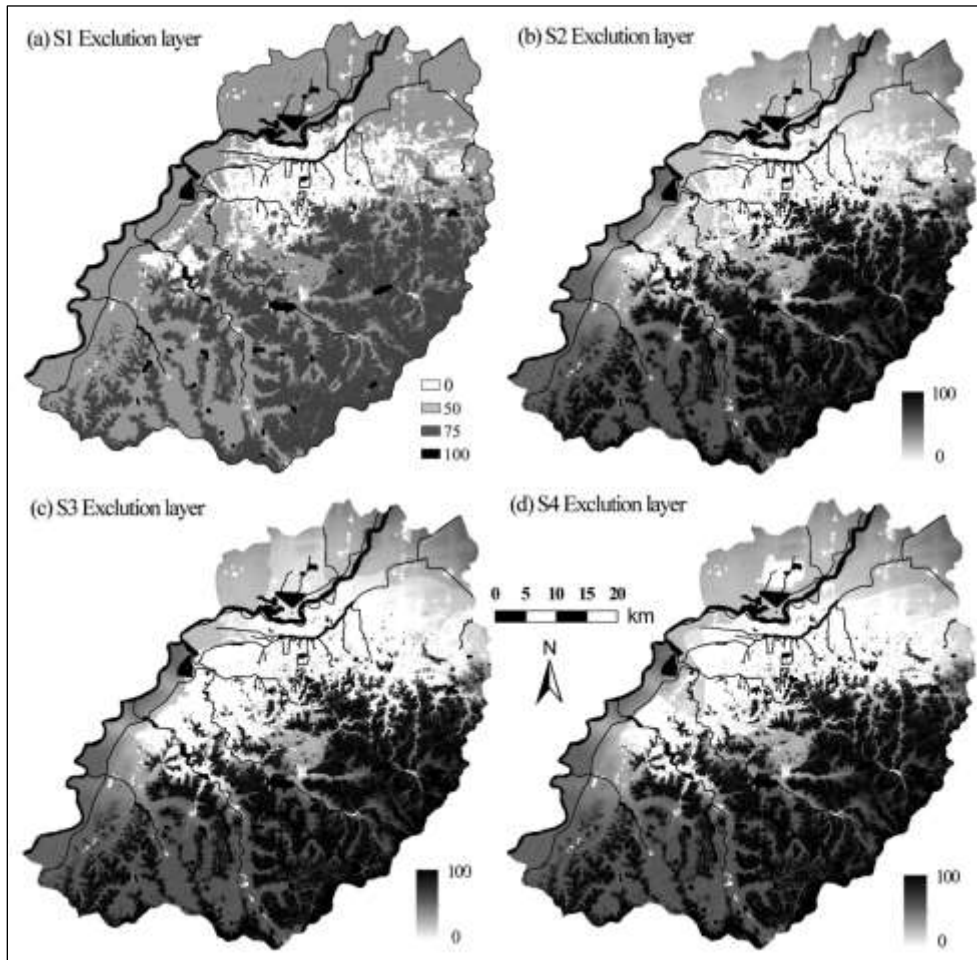
361 The 1996 data were used as the initial layers, while the existing urban extents of 2001, 2006,
362 and 2011 were used for model calibration. Coefficient calibration was carried out under the five
363 designed scenarios using their respective exclusion layers. During the coarse and fine calibration
364 steps, data were resampled into 240 m × 240 m and 120 m × 120 m pixels using five and seven
365 Monte Carlo iterations, respectively. The OSM was calculated in each phase of the model
366 calibration, with the results with the ten highest OSM values selected to determine the optimum
367 combination of the five coefficients for narrowing down the coefficient range, thereby generating
368 five new coefficient ranges. In the final calibration, nine Monte Carlo iterations were performed
369 to extract the five optimum coefficient combinations with the highest OSM values, after which the
370 command “Derive” was executed with a step length of one. One hundred Monte Carlo iterations
371 were used to generate the five final coefficients.

372 The final calibrated coefficients were then used to initialize the prediction module and
373 generate a simulated urban development probability map for 2011. The urbanization thresholds on
374 the probability maps under the respective scenarios were set based on the fact that the urban land
375 use had increased by 285.89 km² during 1996–2011, so any cells with probabilities greater than
376 this threshold value were considered to be the urban areas. To quantify the model simulation
377 accuracy, a comparative analysis between the simulated and remote sensing-derived 2011 urban
378 extent was performed on a pixel scale.

379 **3.5. Model predictions and validation**

380 The model predictions based on the exclusion layers under Scenarios S1–S4 were validated
381 against the 2011 urban land-use map (Fig. 10) (under Scenario S0, the exclusion layer remained
382 unchanged from that in the actual map). Using the 2011 urban extent, exclusion layers, slope
383 gradients, hill shading, and 2011 and 2030 roadway networks as initial input data, 100 Monte Carlo
384 iterations were performed in the model’s prediction mode. The method described in Section 3.4
385 was then used to obtain urban growth simulation results for 2016 and 2040 under the five specified
386 scenarios. The thresholds (88% for S0, 30% for S1, 75% for S2, and 85% for S3 and S4) used in

387 the urbanization probability maps for these scenarios were the same as those in the model
388 calibration stage and were used to reconstruct the urban extent in 2016 and 2040. To examine the
389 zoning scenario impacts, the predicted 2016 maps under the respective scenarios were compared
390 with the 2016 urban extent map derived by remote sensing.



391
392 Fig. 10 Exclusion layers used for simulations under Scenarios 1–4. Note that pixels with attribute
393 values of 100 represent completely excluded areas

394 4. Results

395 4.1. Historical urban growth during 1996–2016

396 The urban extent in the study area grew rapidly from 1996 to 2016 (Fig. 2). During 1996–
397 2001, the urban expansion primarily involved sprawling and infilling (new growth occurring

398 through infilling of free spaces within the developed area) growth at the urban edges. Note that
399 there was nearly no growth in the urban center, primarily because of the implementation of the
400 “Great Changes of Jinan in Five Years” policy (1997–2002) that aimed to enhance the old town
401 and improve the city center environment (Jinan Municipal Planning Bureau, 1997). During 2001–
402 2006, the rapid urban growth primarily occurred in the centers and edges of the new urban areas.
403 For example, in Fig. 2 regions A, D, F, and G exhibit generally spread patterns of these new growth
404 centers, whereas B, C, and E show typical edge-growing patterns. These regions all correspond to
405 the functional groups identified in the Development Plans for the East Metro and West Metro
406 districts since 2003. During 2006–2016, urban growth again comprised primarily edge sprawling
407 and infilling in the newly developed district centers (A–G). These newly developed urban centers
408 saw a rapid development of road networks and accessibility as a result of policy support. The
409 historical urban growth progress appears to be closely related to the development policies. The
410 2011–2030 Jinan master plan specified the promotion of development in the East Metro and West
411 Metro districts, the Jibei Metro area, and the airport development district; these areas are likely to
412 be the primary urban growth areas, and the new planning policies are likely to induce a resumed
413 period of rapid urban growth in Jinan.

414 **4.2. Model calibration results under different scenarios**

415 The data in Table 4 show that each of the seven calibration metrics for the five scenarios is
416 above 0.79, indicating an overall satisfactory simulation performance. The OSM metrics from
417 Scenarios S0 to S4 gradually increase, indicating an improving overall simulation performance,
418 although the improvements among S2, S3, and S4 are all quite limited. The Xmean and Ymean
419 metrics of Scenarios S2, S3, and S4 are significantly higher than those for S0 and S1, indicating
420 better performance in simulating the final urban spatial distribution. The Cluster and Edge metrics
421 increase from Scenarios S0 to S4, indicating that the urban cluster and edge development are also
422 well simulated. The variations seen in the calibration metrics suggest that zoning can affect overall
423 simulation accuracy.

424 **Table 4** Summary of calibration metrics for different scenarios

Scenarios	Calibration metrics							
	Compare	Pop	Edges	Cluster	Slope	Xmean	Ymean	OSM
S0	0.8183	0.9426	0.8807	0.8790	0.9664	0.8144	0.8105	0.3809
S1	0.8174	0.9368	0.8807	0.8807	0.9413	0.8815	0.7933	0.3916
S2	0.8018	0.9219	0.9100	0.9089	0.9108	0.8766	0.9982	0.4872
S3	0.8184	0.9192	0.9147	0.9139	0.9278	0.9009	0.9280	0.4877
S4	0.8342	0.9194	0.9175	0.9126	0.9250	0.9017	0.9181	0.4957

425

426 The final calibration coefficients differ significantly among the five scenarios (Table 5). Each
 427 of the diffusion coefficient values exceeds 98, indicating a clear spontaneous growth pattern. The
 428 breed coefficient for Scenario S0 is 48, as compared to 90 and 96 for Scenarios S3 and S4, and
 429 100 for Scenarios S1 and S2, respectively. This indicates that zoning affected the simulation results
 430 in terms of growth of new urban centers. Each of the spread values is greater than 85, indicating
 431 that the simulations all accurately captured edge growth. The slope coefficient value in Scenario
 432 S0 is 21 but is 1 for the other four scenarios, suggesting that slope had a limited impact on urban
 433 growth, which is potentially partially attributable to the fact that, during 1996–2011 most urban
 434 growth occurred in low slope areas or because the impact of terrain had been considered in
 435 generating the exclusion layers. The road gravity coefficient values are all larger than 56,
 436 indicating that the road network significantly affected urban growth. However, the values
 437 gradually decrease from Scenarios S0 to S4, suggesting that zoning weakened road-influenced
 438 urban growth.

439

440 **Table 5** Final coefficients for respective scenarios

Scenarios	Diffusion	Breed	Spread	Slope	Road gravity
S0	98	48	95	21	90
S1	100	100	85	1	89
S2	100	100	100	1	85
S3	100	90	100	1	61

S4	100	96	100	1	56
----	-----	----	-----	---	----

441

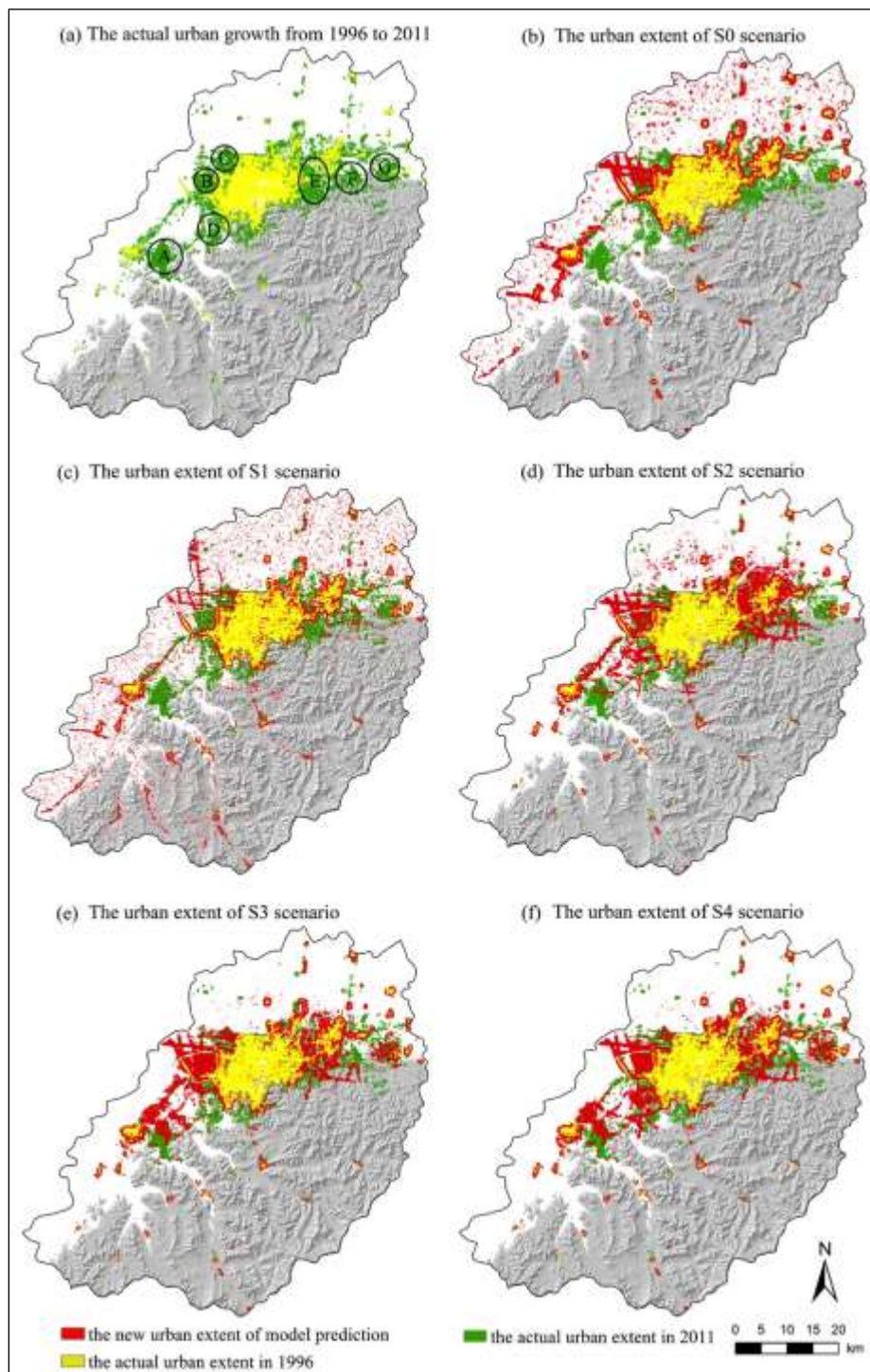
442 **Table 6** Accuracy assessments of 2011 predictions under different scenarios

Scenarios	Nonurban	Urban	New urban	Overall accuracy (%)	
S0	Status as of 2011	826200	131060	79414	–
	Modeled pixels	826708	130552	78906	–
	Number of correct pixels	775769	80137	28491	89.41
	Producer accuracy (%)	93.89	61.15	35.88	–
S1	User accuracy (%)	93.84	61.38	36.11	–
	Modeled pixels	826419	130841	79195	–
	Number of correct pixels	774356	78956	27310	89.14
	Producer accuracy (%)	93.73	60.24	34.39	–
S2	User accuracy (%)	93.70	60.34	34.48	–
	Modeled pixels	821302	135958	84312	–
	Number of correct pixels	781716	91490	39844	89.90
	Producer accuracy (%)	94.62	69.81	50.17	–
S3	User accuracy (%)	95.18	67.29	47.26	–
	Modeled pixels	826853	130407	78761	–
	Number of correct pixels	789028	93156	41510	92.16
	Producer accuracy (%)	95.50	71.08	52.27	–
S4	User accuracy (%)	95.43	71.43	52.70	–
	Modeled pixels	825639	131621	79975	–
	Number of correct pixels	789553	93990	42344	92.19
	Producer accuracy (%)	95.56	71.72	53.32	–
	User accuracy (%)	95.63	71.41	52.95	–

443

444 Comparative analysis at the pixel level between the simulated 2011 urban extent and the urban
445 extent derived from remote sensing reveals overall accuracies of above 89% for all scenarios, with
446 a small but persistent increase from Scenarios S0 to S4 (except for Scenario S1) (Table 6). The
447 results indicate that the model performed better under zoning scenarios S2, S3, and S4 than under
448 the non-zoning (S0) or simplified zoning (S1) scenarios. Except for Scenario S1, the producer
449 accuracy increases by 10.57% from S0 to S4, with the user accuracy following a similar trend.
450 However, the simulation accuracy for predicting newly urbanized pixels between 1996 and 2011
451 increases by only about 17% from S0 to S4, suggesting that the zoning scheme based on land-use

452 type (S1) barely helped to improve the simulation accuracy, although the other three zoning
453 schemes (S2–S4) did help boost the model’s capability in this regard. Nevertheless, it was still
454 quite difficult to accurately model newly urbanized areas.



455

456 Fig. 11 Existing (a) and simulated (b-f) urban extents in 2011 under different scenarios.

457

458 Further comparison of the simulated and remote sensing-derived 2011 urban extent (Fig. 11)
459 reveals that, under Scenarios S0 and S1, the model performed well in projecting urban growth
460 along edges and roads but not very well in predicting clustered growth (Fig. 11b, c). This suggests
461 that when zoning is not considered or is represented in a simplified manner (as in Scenario S1), it
462 is difficult to accurately reproduce the clustered growth that can be spurred by urban development
463 policies or strategies. Even though spatial growth along urban edges and roads remains the
464 dominant pattern under zoning scenarios S2–S4, clustered growth and newly urbanized centers
465 begins to rise in varied patterns across Regions A–G (Fig. 11d-f). For example, the clustered
466 growth in Regions A, C, and G under Scenario S2 was much smaller than under Scenarios S3 and
467 S4. Compared with the other scenarios, S3 and S4 yielded the most extensive clustered growth,
468 closely matching the urban growth patterns revealed by remote sensing. This suggests that
469 appropriate zoning schemes can help improve model performance in projecting the clustered urban
470 growth that can be spurred by development policies and strategies.

471 **4.3. Urban growth predictions under different zoning scenarios**

472 Two snapshots (2016 and 2040) of predicted urban growth were generated and the remote
473 sensing-derived and modeled urban extents of 2016 were compared to examine the impacts of
474 zoning scenario on urban growth simulation accuracy. The 2016 simulation accuracies obtained
475 using the selected metrics for the respective scenarios (Table 7) follow trends similar to those of
476 2011 (Table 6). Specifically, identical to the 2011 results a high level of overall accuracy
477 (universally greater than 96%) was achieved by using the calibrated SLEUTH model to predict the
478 urban growth in 2016 under each scenario. Except for Scenario S1, the overall accuracy gradually
479 increased from Scenarios S0 to S4 (Table 7), suggesting that the model performed better under the
480 latter three zoning scenarios than under the non-zoning (S0) or simplified (S1) zoning scenarios.
481 The producer and user accuracies of the simulated non-urban and urbanized areas for 2016 were
482 all higher than those for 2011 but lower for the simulated newly urbanized area (Tables 6, 7). A

483 comparison of the 2011 and 2016 newly urbanized pixels (Fig. 12) reveals a decrease from 79,414
 484 to 14,862 pixels over this period with a corresponding reduction in the number of clustered growth
 485 areas. The lower accuracy for the newly urbanized areas suggests that the simulation was more
 486 difficult for such areas than for other (non-urban and urban) areas. These results indicate that some
 487 newly urbanized areas developed primarily in conjunction with the implementation of urban
 488 planning policies, although the decrease in the impacts of zoning on projected urban growth might
 489 have contributed to the observed reduced producer and user accuracies.

490 **Table 7** Assessment of the accuracy of 2016 predictions under different scenarios

Scenarios		Nonurban	Urban	New urban	Overall accuracy (%)
S0	Status as of 2016	811338	145922	14862	–
	Modeled pixels	817204	140056	8996	–
	Number of correct pixels	804080	132798	1738	97.87
	Producer accuracy (%)	99.11	91.01	11.69	–
	User accuracy (%)	98.39	94.81	19.32	–
S1	Modeled pixels	798999	158261	27201	–
	Number of correct pixels	788527	135450	4390	96.52
	Producer accuracy (%)	97.19	92.82	29.54	–
	User accuracy (%)	98.69	85.59	16.14	–
S2	Modeled pixels	804314	152946	21886	–
	Number of correct pixels	793864	135172	4112	97.05
	Producer accuracy	97.85	92.63	27.67	–
	User accuracy (%)	98.70	88.38	18.79	–
S3	Modeled pixels (%)	806193	151067	20007	–
	Number of correct pixels	795489	135218	4158	97.23
	Producer accuracy (%)	98.05	92.66	27.98	–
	User accuracy (%)	98.67	89.51	20.78	–
S4	Modeled pixels	806413	150847	19787	–
	Number of correct pixels	795702	135211	4151	97.25
	Producer accuracy (%)	98.07	92.66	27.93	–
	User accuracy (%)	98.67	89.63	20.98	–

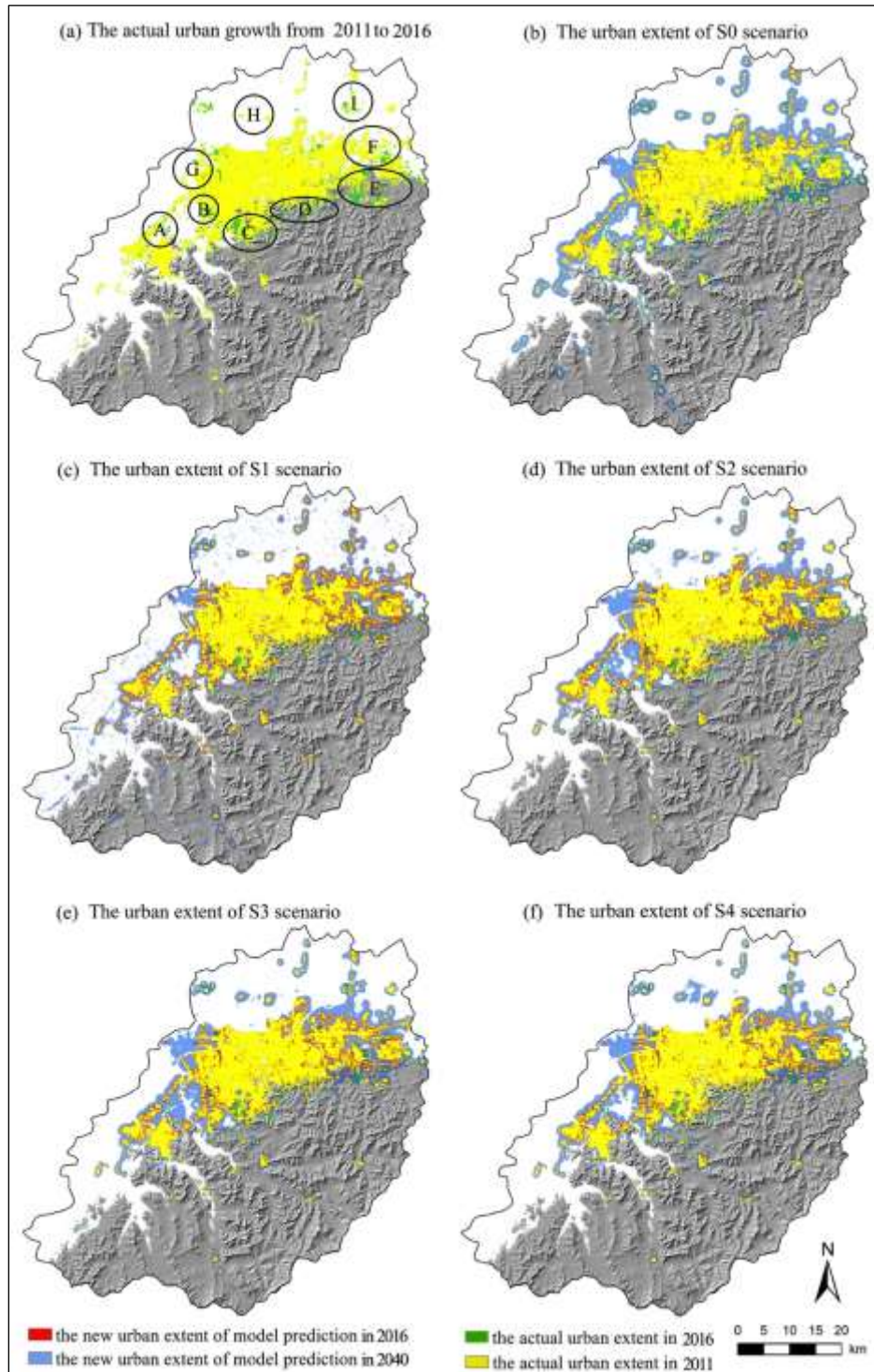
491

492 The predicted urban extent for 2040 indicates that the simulated urban growth under Scenario
493 S0 is primarily characterized by edge and infilling development (Fig. 12b), reflecting the patterns
494 observed during the calibration stage. The model output map shows that the urban growth within
495 Regions A–F, H, and I comprised primarily edge growth without significant clustered growth (Fig.
496 12b). This result might be related to the fact that the state of a cell within the SLEUTH model
497 depends significantly on the state of its neighboring cells; thus, an existing urban cell will tend to
498 expand outward rapidly, but the spread of new growth center tend to be slower (Akin et al., 2014;
499 Jantz et al., 2003, 2010). Scenario S1 also shows an obvious edge growth pattern (Fig. 12c), which
500 indicates that the model still cannot capture future clustered growth caused by regional
501 differentiation of urban development policies despite the consideration of land-use type-based
502 zoning.

503 The clustered growth in Zones A, B, F, and G under Scenarios S2, S3, S4 was significantly
504 greater than under S0 and S1 (Fig. 12), indicating that the model is able to incorporate zoning
505 information into urban development and differentiate urban growth within various zones
506 accordingly. Relative to the other four scenarios, S4 produced the most clustered growth in Zone
507 H (the center of the Jibei Metro area) (Fig. 12f), suggesting that zoning based on development
508 planning can help effectively project clustered development stimulated by urban development
509 policies and strategies.

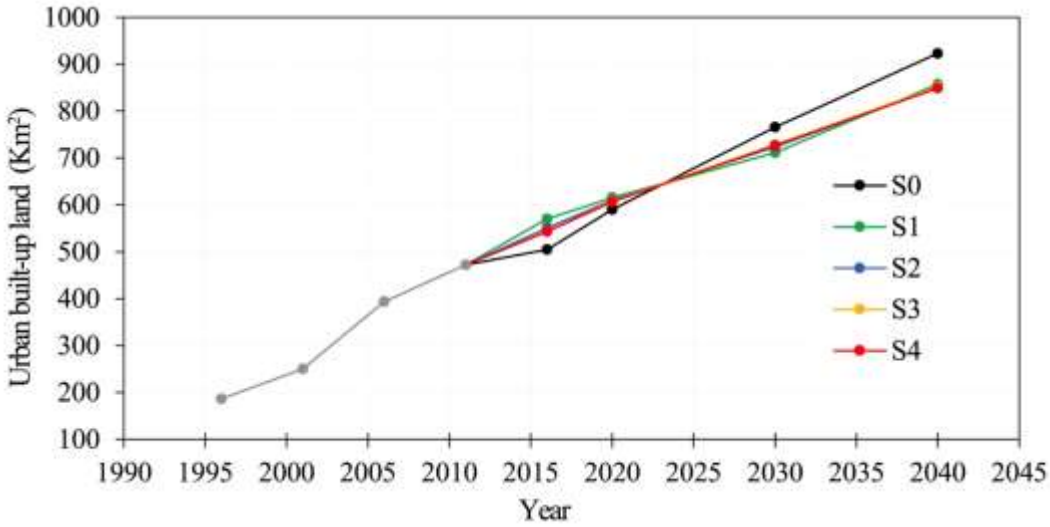
510 The data in Fig. 13 indicate that the urban area is predicted to grow quickly during 2011–2040
511 under all five scenarios, with Scenario S0 producing among the fastest urban growth. Under this
512 scenario, the urbanized area increases by 451 km² at an annual growth rate of 2.34%. By
513 comparison, Scenario S4 produces the least urban growth, with an urbanized area increasing by
514 only 377 km² at an annual growth rate of 2.05%. The projected urban growth areas under Scenarios
515 S1–S3 are all slightly larger than under Scenario S4 and differ significantly from S4 during 2012–
516 2020. This indicates that Scenario S0, which does not incorporate any zoning scheme, projects a
517 higher rate of urbanization than Scenarios S1–S4. These findings suggest that designing specific

518 zoning scenarios based on spatial differentiation and growth management policies can help not
 519 only in revealing the impacts of different zoning scenarios on urban growth simulation results but
 520 also improve performance in predicting future urban growth.



521
 522 Fig. 12 Simulated urban extents in 2016 and 2040 under different scenario s: (a) actual and (b-f)

523 modeled urban growth.



524

525 Fig. 13 Growth of urban built-up land during 2011–2040 under the five scenarios

526

527 5. Discussion and Conclusions

528 In this study, the city of Jinan, China was used as a case study to demonstrate the potential
529 impacts of planning policies and strategies on urban growth prediction patterns and accuracy using
530 a cellular-automaton-based urban growth model. To date, it has been difficult to integrate planning
531 policies into the conversion rules used by the SLEUTH model (Torrens, 2011), and many case
532 studies have indicated that this model could not effectively characterize the potential impacts of
533 urban development policies on urban land use (Clarke et al., 1997; Silva and Clarke, 2002; Lahti,
534 2008; Wu et al., 2009). However, we found that using an appropriate method to incorporate zoning
535 can help improve simulation accuracy and therefore the capability of simulating the effects of
536 urban development policies (Chaudhuri and Clarke, 2013; Akin et al., 2014; Onsted and
537 Chowdhury, 2014).

538 Four zoning scenarios (S1–S4,) as well as a scenario that did not include zoning (S0), were
539 developed through the generation of different types of exclusion layers. The SLEUTH 3.0 model
540 was used to simulate urban growth in 2011, 2016, and 2040 under various scenarios and the results

541 were assessed at the pixel level. The main conclusions are as follows. (1) At the pixel level, overall
542 accuracy is not quite meaningful in representing model accuracy; instead, producer or user
543 accuracy of newly urbanized pixels might be more appropriate. (2) Incorporating planning policies
544 into zoning information can help improve the prediction accuracy of newly urbanized pixels, better
545 represent clustered development, and boost the level of spatial matching, while zoning based on
546 land-use type does not offer such improvements. (3) Compared with the no-zoning scenario (S0),
547 the scenario in which zoning was based on development planning subdivisions (S4) generated the
548 largest improvement in the prediction accuracy, followed by scenarios S3, S2, and S1. Using the
549 city of Jinan as a case study, the study demonstrated that more detailed (i.e., more finely divided)
550 zoning, particularly in areas with high probability of urban growth, can yield more accurate
551 predictions. The scenarios taking into account the spatial differentiation of development planning
552 policies (S2–S4) generated better predictions than the scenario considering land-use type only (S1),
553 as the former scenarios incorporated more finely divided zoning schemes. In a summary,
554 incorporating zoning information based on spatial differentiation and growth management policies
555 can help improve simulation accuracy and spatial matching degree, thus allowing the more
556 accurate projection of urbanizing patterns through the use of appropriately designed zoning
557 schemes.

558 Although a number of previous studies examined the impacts of zoning on simulation
559 accuracy (e.g., [White and Engelen, 1993](#); [Berling-Wolff and Wu, 2004](#); [Onsted and Chowdhury,](#)
560 [2014](#)), the potential impact of different zoning schemes on simulation accuracy has not been
561 thoroughly investigated. For example, [Berling-Wolff and Wu \(2004\)](#) considered agricultural land
562 to be a separate category in simulating the urban landscape dynamics of the city of Phoenix in the
563 United States in an approach similar to that used in other studies that did not consider zoning
564 information ([Jantz et al., 2003, 2010](#); [Rafiee et al., 2009](#); [Akin et al., 2014](#)). Models in which
565 various protection levels (or conversion probabilities) were assigned to different land-use types
566 based on urban development policies have proven capable of capturing the spatial consequence of

567 urban development policies. [Onsted and Chowdhury \(2014\)](#) considered three types of zoning, i.e.,
568 developmental, interim, and agricultural zoning, using various zoning assignment methods and
569 evaluated the model accuracy variation in terms of the amounts or rates of urban growth under
570 different assignment methods using the OSM metric. Unlike these previous studies, this study
571 explored the impacts of several zoning schemes based on land-use type, urbanized suitability,
572 administrative division, and planning subdivision (functional groups), with the prediction accuracy
573 evaluated at the pixel level using the OSM metric. Our findings should be useful in improving the
574 performance of urban growth predictions through the use of appropriately designed zoning
575 scenarios.

576 However, several issues may require further attention. First, an alternative weighting method
577 might help better capture the zoning information within a model, as the demand on urban land use
578 in different areas often varies ([Goldstein et al., 2004](#)) and land-use change can be significantly
579 influenced by local land-use policies. Under Scenarios S3 and S4, the development policy impact
580 coefficient layer was used to indicate the impact of development policies on regional differences
581 in urban growth using a user-defined option. However, the relationship among different levels of
582 development policy is usually difficult to quantify precisely, and therefore the values of policies at
583 various levels requires further testing. Second, further research is required on choosing an
584 appropriate zoning scale, as this can significantly affect the simulation outcome. A study conducted
585 by [Wu et al. \(2009\)](#) on the Shenyang Metropolitan area found that the SLUETH model did not
586 perform well when modeling a zoning scheme with large administrative districts (~700 km²). In
587 our study, the use of more detailed zoning schemes in conjunction with development policy, such
588 as the schemes in Scenarios S3 and S4 based on administrative districts (av. 57.43 km²) and
589 development functions (av. 41.02 km²), respectively, helped boost the simulation accuracy.
590 Similarly, the scheme used for S2 featuring more detailed zoning granularity but not considering
591 spatial differences in development policy yielded moderate simulation accuracy. Thus, further

592 research is needed to examine the development policy effects of scale on simulation accuracy
593 through the application of measurable weighting methods under various zoning schemes.

594 **References**

- 595 Aburas, M. M., Ho, Y. M., Ramli, M. F., Ash'aari, Z. H. (2016). The simulation and prediction of
596 spatio-temporal urban growth trends using cellular automata models: A review. *International*
597 *Journal of Applied Earth Observation and Geoinformation*, 52: 380-389.
- 598 Arsanjani, J. J., Helbich, M., Kainz, W., Boloorani, A. D. (2013). Integration of logistic regression,
599 Markov chain and cellular automata models to simulate urban expansion. *International*
600 *Journal of Applied Earth Observation and Geoinformation*, 21: 265-275.
- 601 Akın, A., Clarke, K. C., Berberoglu. (2014). The impact of historical exclusion on the calibration
602 of the SLEUTH urban growth model. *International Journal of Applied Earth Observation and*
603 *Geoinformation*, 27:156-168.
- 604 Al-shalabi, M., Billa, L., Pradhan, B. (2012). Modelling urban growth evolution and land-use
605 changes using GIS based cellular automata and SLEUTH models: the case of Sana'a
606 metropolitan city, Yemen. *Environmental Earth Sciences*, 70:425-437.
- 607 Berling-Wolff, S., Wu, J. (2004). Modeling urban landscape dynamics: a case study in Phoenix,
608 USA. *Urban Ecosystems*, 7: 215-240.
- 609 Brown, D. G., Band, L. E., Green, K. O., Irwin, E. G., Jain, A., Lambin, E. F., Pontius Jr, R. G.,
610 Seto, K. C., Turner II, B.L., Verburg, P. H. (2013). *Advancing land change modeling:*
611 *opportunities and research requirements.* The National Academies Press, Washington DC.
- 612 Chaudhuri, G., Clarke, K. C. (2013). How does land use policy modify urban growth? A case study
613 of the Italo-Slovenian border. *Journal of Land Use Science*, 8(4):443-465.
- 614 Chowdhury, P. R., Maithani, S. (2014). Modelling urban growth in the Indo-Gangetic plain using
615 nighttime OLS data and cellular automata. *International Journal of Applied Earth*
616 *Observation and Geoinformation*, 33: 155-165.
- 617 Clarke, K. C., Gaydos, L. J. (1998). Loose coupling a cellular automaton model and GIS: long-
618 term urban growth Prediction for San Francisco and Washington/Baltimore. *International*
619 *Journal of Geographical Information Science*, 12: 699-714.

620 Clarke, K. C., Hoppen, S., Gaydos, L. (1997). A self-modifying cellular automaton model of
621 historical urbanization in the San Francisco Bay area. *Environment and Planning B: Planning
622 and Design*, 24:247-261.

623 Dalvi, M. Q., Martin, K. M. (1976). The measurement of accessibility: some preliminary results.
624 *Transportation*, 5:17-42.

625 Dietzel, C., Clarke, K. C. (2007). Toward Optimal Calibration of the SLEUTH Land Use Change
626 Model. *Transactions in GIS*, 11:29-45.

627 Geurs, K. T., Van Wee, B. (2004). Accessibility evaluation of land-use and transport strategies:
628 review and research directions. *Journal of Transport geography*, 12(2): 127-140.

629 Goldstein, N. C., Candau J. T., Clarke, K. C. (2004). Approaches to simulating the “March of
630 Bricks and Mortar”. *Computers, Environment and Urban Systems*, 125-147.

631 Hansen, W. G. (1959). How accessibility shapes land use. *Journal of American Institute of Planners*,
632 25 (1): 73-76.

633 Herold, M., Goldstein, N. C., Clarke, K. C. (2003). The spatiotemporal form of urban growth:
634 measurement, analysis and modeling. *Remote sensing of Environment*, 86: 286-302.

635 Hu, Z., Lo, C. P. (2007) Modeling urban growth in Atlanta using logistic regression. *Computers
636 Environment and Urban Systems*, 31 (6): 667-688.

637 Irwin, E. G., Jayaprakash, C., Munroe, D. K. (2009). Towards a comprehensive framework for
638 modeling urban spatial dynamics. *Landscape Ecology*, 24(9): 1223-1236.

639 Jantz, C. A., Goetz, S. J., Donato, D. (2010). Designing and implementing a regional urban
640 modeling system using the SLEUTH cellular urban model. *Computers, Environment and
641 Urban Systems*, 34: 1-16.

642 Jantz, C. A., Goetz, S. J., Shelley, M. K. (2003). Using the SLEUTH urban growth model to
643 simulate the impacts of future policy scenarios on urban land use in the Baltimore-
644 Washington metropolitan area. *Environment and Planning B: Planning and Design*, 30: 251-
645 271.

646 Jinan Municipal Planning Bureau. (2006). Master Planning of Jinan City (2006-2020), Jinan (in
647 Chinese).

648 Jinan Municipal Planning Bureau. (2007). Great Changes of Jinan in Five Years (1997–2002),
649 Jinan (in Chinese).

650 Kong, F. H., Yin, H. W., Nakagoshi, N., James, P. (2012). Simulating urban growth processes
651 incorporating a potential model with spatial metrics. *Ecological Indicators*, 20: 82-91.

652 Ku, C. A. (2016). Incorporating spatial regression model into cellular automata for simulating land
653 use change. *Applied Geography*, 69, 1-9.

654 Lahti, J. (2008). Modelling urban growth using cellular automata: a case study of Sydney, Australia.
655 Enschede, The Netherlands: International Institute for Geo-Information Science and Earth
656 Observation (MA thesis).

657 Liu, T., Yang, X. (2015). Land change modeling: status and challenges. In *Monitoring and
658 Modeling of Global Changes: A Geomatics Perspective* (pp. 3-16). Springer Netherlands.

659 Liu, W., Seto, K. (2008). Using the ART-MMAP neural network to model and predict urban growth:
660 a spatiotemporal data mining approach. *Environment and Planning B-Planning & Design*, 35
661 (2): 296-317.

662 Liu, X., Li, X., Shi, X. (2008). Simulating complex urban development using kernel-based non-
663 linear cellular automata. *Ecological Modelling*, 211:169-181.

664 Long, Y., Gu, Y., Han, H. (2012). Spatiotemporal heterogeneity of urban planning implementation
665 effectiveness: Evidence from five urban master plans of Beijing. *Landscape and Urban
666 Planning*, 108:103-111.

667 Ma, L., Guo, J., Velthof, G. L., Li, Y., Chen, Q., Ma, W., Oenema, O. and Zhang, F. (2014). Impacts
668 of urban expansion on nitrogen and phosphorus flows in the food system of Beijing from
669 1978 to 2008. *Global Environmental Change*, 28:192-204.

670 Mahiny, A. S., Clarke, K. C. (2012). Guiding SLEUTH land-use/land-cover change modeling
671 using multicriteria evaluation: towards dynamic sustainable land-use planning. *Environment*
672 *and Planning B: Planning and Design*, 39: 925-944.

673 Maimaitijiang, M., Ghulam, A., Sandoval, J. O., Maimaitiyiming, M. (2015). Drivers of land cover
674 and land use changes in St. Louis metropolitan area over the past 40 years characterized by
675 remote sensing and census population data. *International Journal of Applied Earth*
676 *Observation and Geoinformation*, 35: 161-174.

677 Matthews, R., Gilbert, N., Roach, A., Polhill, J., Gotts, N. (2007). Agent-based land-use models:
678 a review of applications. *Landscape Ecology*, 22:1447–1459.

679 Onsted, J. A., Chowdhury, R. R. (2014). Does zoning matter? A comparative analysis of landscape
680 change in Redland, Florida using cellular automata. *Landscape and Urban Planning*, 121: 1-
681 18.

682 Rafiee, R., Mahiny, A. S., Khorasanic, N. (2009). Simulating urban growth in Mashad City, Iran
683 through the SLEUTH model (UGM). *Cities*, 26:19-26.

684 Saaty, T. L. (1980). *The Analytic Hierarchy Process: Planning, Priority Setting, Resource*
685 *Allocation*. McGraw Hill, New York.

686 Shafizadeh-Moghadam, H., Helbich, M. (2015). Spatiotemporal variability of urban growth
687 factors: A global and local perspective on the megacity of Mumbai. *International Journal of*
688 *Applied Earth Observation and Geoinformation*, 35: 187-198.

689 Silva, E. A., Ahern, J., Wileden, J. (2008). Strategies for landscape ecology: An application using
690 cellular automata models. *Process in Planning*, 70:133-177.

691 Silva, E. A., Clarke, K. C. (2002). Calibration of the SLEUTH urban growth model for Lisbon and
692 Porto, Portugal. *Computers, Environment and Urban Systems*, 26: 525-552.

693 Song, W., Pijanowski, B. C., Tayyebi, A. (2015). Urban expansion and its consumption of high-
694 quality farmland in Beijing, China. *Ecological Indicators*, 54: 60-70.

695 *Statistical Year Book of Jinan*. (2015). Beijing: China Statistics Press (in Chinese).

696 The Yearbook of China's Cities. (2015). Beijing: China Statistics Press (in Chinese).

697 Tian, L., Shen, T. (2011). Evaluation of plan implementation in the transitional China: A case of
698 Guangzhou city master plan. *Cities*, 28:11-27.

699 Torrens, P. M. (2002). *SprawlSim: modeling sprawling urban growth using automata-based models.*
700 *Agent-based models of land-use and land-cover change.* LUCC International Project Office,
701 Belgium, 72-79.

702 Torrens, P. M. (2011). Calibrating and validating cellular automata models of urbanization. In
703 *Urban remote sensing: Monitoring, synthesis and modeling in the urban environment*, 335-
704 345.

705 Valbuena, D., Verburg, P., Bregt, A., Ligtenberg, A. (2010). An agent-based approach to model
706 land-use change at a regional scale. *Landscape Ecology*, 25(2): 185–199.

707 White, R. W., Engelen, G. (1993). Cellular automata and fractal urban form: a cellular modeling
708 approach to the evolution of urban land use patterns. *Environment and Planning A*, 25:1175-
709 1193.

710 Wu, X., Hu, Y., He, H. (2009). Performance Evaluation of the SLEUTH Model in the Shenyang
711 Metropolitan Area of Northeastern China, *Environmental Modeling and Assessment*, 14(2):
712 221-230.

713 Yang, X., Lo, C. P. (2003). Modeling urban growth and landscape changes in the Atlanta
714 metropolitan area. *International Journal of Geographical Information Science*, 17: 463-488.

715 Yin, H. W., Kong, F. H., Hu, Y. M., Philip, J., Xu, F., Yu, L. J. (2015). Assessing Growth Scenarios
716 for their Landscape Ecological Security Impact, using the SLEUTH Urban Growth Model.
717 *Journal of Urban Planning and Development*, 142(2): 05015006.

718 Yu, X. J., Ng, C. N. (2007). Spatial and temporal dynamics of urban sprawl along two urban–rural
719 transects: A case study of Guangzhou, China. *Landscape and Urban Planning*, 79(1): 96-109.

720

721 **Table list**

722 [Table 1](#) Data layers used in the multi-factor overlay analysis for urbanized suitability assessment
723 and the weights assigned to each of the seven factors

724 [Table 2](#) List of major urban and regional development policies for Jinan since 1996 and their
725 respective policy levels

726 [Table 3](#) Description of metrics used for evaluation of the calibration results

727 [Table 4](#) Summary of calibration metrics for different scenarios

728 [Table 5](#) Final coefficients for respective scenarios

729 [Table 6](#) Accuracy assessments of 2011 predictions under different scenarios

730 [Table 7](#) Accuracy assessment of 2016 prediction under different scenarios

731

732 **Figure list**

733 [Fig. 1](#) Location of the study area

734 [Fig. 2](#) Spatial growth of urban extent in Jinan from 1996 to 2016. A-G: components of urban
735 growth regions

736 [Fig. 3](#) Road networks for 1996, 2001, 2006, and 2011

737 [Fig. 4](#) Two model input layers: slope (a) and hillshade (b)

738 [Fig. 5](#) Exclusion layers used for Scenarios S0 (a) and S1 (b). Note that pixels with the attribute
739 value of 100 represent completely excluded areas

740 [Fig. 6](#) Four factors used in the multi-factor overlay analysis for urbanized suitability assessment

741 [Fig. 7](#) Accessibility factors used in the multi-factor overlay analysis for urbanized suitability
742 assessment and the exclusion layer used in Scenario S2

743 [Fig. 8](#) Administrative division-based development policy impact coefficient layer (a) and
744 exclusion layer used in Scenario S3 (b). Note that pixels with attribute values of 100 represent
745 completely excluded areas

746 [Fig. 9](#) Functional group-based development policy impact coefficient layer (a) and exclusion layer
747 used in Scenario S4 (b). Note that pixels with attribute values of 100 represent completely
748 excluded areas

749 [Fig. 10](#) Exclusion layers used for simulations under Scenarios 1–4. Note that pixels with attribute
750 values of 100 represent completely excluded areas

751 [Fig. 11](#) Existing (a) and simulated (b-f) urban extents in 2011 under different scenarios

752 [Fig. 12](#) Simulated urban extents in 2016 and 2040 under different scenarios: (a) actual and (b-f)
753 modeled urban growth

754 [Fig. 13](#) Growth of urban built-up land during 2011–2040 under the five scenarios

755